LETTER

Quantum gates and memory using microwave–dressed states

N. Timoney[1], I. Baumgart[1], M. Johanning[1], A. F. Varón[1], M. B. Plenio[2], A. Retzker[2] & Ch. Wunderlich[1]

Trapped atomic ions have been used successfully to demonstrate[1] basic elements of universal quantum information processing. Nevertheless, scaling up such methods to achieve large-scale, universal quantum information processing (or more specialized quantum simulations[2–5]) remains challenging. The use of easily controllable and stable microwave sources, rather than complex laser systems[6,7], could remove obstacles to scalability. However, the microwave approach has drawbacks: it involves the use of magnetic-field-sensitive states, which shorten coherence times considerably, and requires large, stable magnetic field gradients. Here we show how to overcome both problems by using stationary atomic quantum states as qubits that are induced by microwave fields (that is, by dressing magnetic-field-sensitive states with microwave fields). This permits fast quantum logic, even in the presence of a small (effective) Lamb–Dicke parameter (and, therefore, moderate magnetic field gradients). We experimentally demonstrate the basic building blocks of this scheme, showing that the dressed states are long lived and that coherence times are increased by more than two orders of magnitude relative to those of bare magnetic-field-sensitive states. This improves the prospects of microwave-driven ion trap quantum information processing, and offers a route to extending coherence times in all systems that suffer from magnetic noise, such as neutral atoms, nitrogen-vacancy centres, quantum dots or circuit quantum electrodynamic systems.

Using laser light for coherent manipulation of quantum bits (qubits) gives rise to fundamental issues, notably unavoidable spontaneous emission that destroys quantum coherence[8,9]. The difficulty of cooling a collection of ions to their motional ground state and the long duration of this process in the presence of spurious heating of Coulomb crystals limits the fidelity of quantum logic operations in laser-based quantum gates and thus hampers scalability. This limitation is only partly removed by the use of 'hot' gates[10,11]. Technical challenges in accurately controlling the frequency and intensity of laser light as well as in targeting a large number of laser beams of high intensity on trapped ions are further obstacles to scalability.

These issues associated with the use of laser light for scalable QIP have led to the development of novel ways of performing conditional quantum dynamics with trapped ions that rely on radio-frequency or microwave radiation instead of laser light[6,7,12–15]. Radio-frequency or microwave radiation can be used in quantum gates through the use of magnetic-gradient-induced coupling between spin states of ions[16], thus averting the technical and fundamental issues of scalability that were described above. Furthermore, the sensitivity to motional excitation of ions is reduced in such schemes. A drawback of magnetic-gradient-induced coupling is the necessity of using magnetic-field-sensitive states for conditional quantum dynamics, thus making qubits susceptible to ambient field noise and shortening their coherence times. This issue is shared with some optical ion trap schemes for QIP that usually rely on magnetic-field-sensitive states for conditional quantum dynamics, such as geometric gates[1], limiting the coherence time of qubit states typically to a few milliseconds. In an effort to extend the coherence times of atomic states, two-qubit entangled states

forming a decoherence-free subspace have been created[17,18]. Recently, transfer between field-sensitive states used for conditional quantum dynamics and field-insensitive states used for storage of quantum information has been utilized[19].

The relevant noise source in this case, namely magnetic field fluctuations, is not featureless white noise but tends to have a limited bandwidth. In this context, techniques were proposed for prolonging coherence times by subjecting the system to a rapid succession of pulses leading to a decoupling from the environment. This technique, termed bang–bang control[20], and its continuous version[21] can be applied usefully in a variety of systems including hybrid atomic physics and nanophysics technologies. Recent work includes the experimental demonstration of optimized pulse sequences made for suppression of qubit decoherence (see refs 22, 23 and references therein).

Here we encode qubits in microwave-dressed states requiring only continuous, constant-intensity microwave fields. This scheme protects qubits from magnetic field fluctuations and, importantly, simultaneously allows fast quantum logic even for small Lamb–Dicke parameters and, therefore, moderate magnetic field gradients. Microwave-generating elements for the coherent manipulation of qubits can be integrated into microstructured ion traps[7] such that QIP can be realized using scalable ion chips. Thus, this novel scheme is a significant step towards the integration of elements required for QIP on a scalable ion chip. Moreover, the ideas presented here are generic and can be applied to all laser- or microwave-based QIP.

We theoretically describe the scheme for storage and single- and multiqubit quantum gate operation, and then present experimental demonstrations of storage and information processing of quantum information that demonstrate gains of more than two orders of magnitude in coherence times over approaches involving bare states.

We consider a typical energy-level configuration (Fig. 1a). Encoding quantum information in the subspace spanned by two magnetically sensitive $m_F = \pm 1$ states, $|-1\rangle$ and $|+1\rangle$, will lead to a rapid loss of coherence owing to fluctuating magnetic fields. We first note that microwave-dressed states create a subspace spanned by the two states $|D\rangle = (|-1\rangle - |+1\rangle)/\sqrt{2}$ (a dark state) and $|0'\rangle$ ($m_F = 0$) of the same manifold. This subspace is separated from the other eigenstates of the system, $|u\rangle$ and $|d\rangle$, by a finite energy gap (the dressing fields' Rabi frequency is denoted by Ω, and $|\Delta_- - \Delta_+| \ll \Omega$ should hold for the detunings Δ_- and Δ_+; refs 24, 25). The energetically degenerate states $|D\rangle$ and $|0'\rangle$ are not coupled by magnetic field fluctuations. As a consequence of the energy gap between these states and the states $|u\rangle$ and $|d\rangle$, a relative phase change between $|-1\rangle$ and $|+1\rangle$ acquires an energy penalty and dephasing is strongly suppressed as long as the spectral power density of the magnetic field fluctuations at the frequency corresponding to the energy gap is negligible. We note that the levels $|D\rangle$ and $|0'\rangle$ are energetically degenerate independent of the applied microwave Rabi frequency, Ω, and are hence stable against its power fluctuations. Therefore, we consider the qubit encoded in the subspace spanned by $|D\rangle$ and $|0'\rangle$. The microwave fields do not couple any states in the qubit subspace and thus do not limit the phase coherence.

[1]Faculty of Science and Technology, Department of Physics, University of Siegen, 57068 Siegen, Germany. [2]Institute for Theoretical Physics, University of Ulm, 89069 Ulm, Germany.
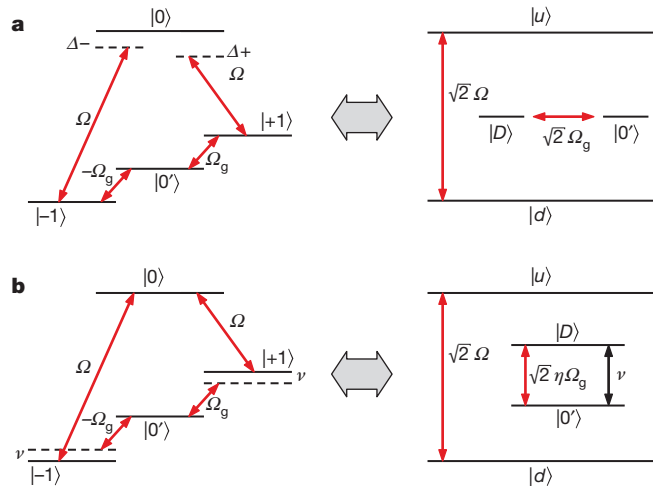
Figure 1 | Microwave-dressed qubit states. Left, atomic states and microwave-dressing fields with Rabi frequency Ω. $|-1\rangle$ and $|+1\rangle$ represent magnetic-field-sensitive states, and have, for instance, $m_F = \pm 1$, and $|0\rangle$ and $|0'\rangle$ represent magnetically insensitive levels (and are, for instance, the $m_F = 0$ states of two different hyperfine manifolds). Right, dressed states. $|D\rangle = (|-1\rangle - |+1\rangle)/\sqrt{2}$ and $|0'\rangle$ are separated by an energy gap from two other states, $|u\rangle = (|B\rangle + |0\rangle)/\sqrt{2}$ and $|d\rangle = (|B\rangle - |0\rangle)/\sqrt{2}$, where $|B\rangle = (|-1\rangle + |+1\rangle)/\sqrt{2}$. Thus, a qubit with states $|D\rangle$ and $|0'\rangle$ is created that is resilient to magnetic field fluctuations and to microwave power fluctuations. **a**, A radio-frequency field with Rabi frequency Ω_g is used to implement general single-qubit quantum gates. **b**, Conditional quantum dynamics coupling electronic degrees of freedom to the motion of trapped atoms is achieved when the radio-frequency field is detuned from the qubit's carrier transition frequency by the vibrational frequency, v.

The nature of the protected subspace depends on the relative phase between the microwave fields on the transitions $|0\rangle \leftrightarrow |\pm 1\rangle$. The above description applies for a relative phase of zero, whereas for a relative phase of π the protected subspace is spanned by $|B\rangle = (|-1\rangle + |+1\rangle)/\sqrt{2}$ and $|0'\rangle$ (Methods). We considered both cases in the experiments reported below.

The application of one or two additional radio-frequency fields with Rabi frequency Ω_g, possible detuning Δ_g and a possible initial relative phase of π (Methods) then permits the implementation of general single-qubit rotations in the protected subspace spanned by $|B\rangle$ and $|0'\rangle$ in the case of one additional field and by $|D\rangle$ and $|0'\rangle$ in the case of two additional fields. Choosing $\Delta_g = 0$ yields the Hamiltonian $H = \Omega_g(|D\rangle\langle 0'| + |0'\rangle\langle D|)$, which in a Bloch-sphere picture describes arbitrary rotations about the x axis in the protected space. A rotation about the z axis is obtained for $\Delta_g \neq 0$ and $\Omega_g \neq 0$ under the conditions $\Omega_g \ll \Delta_g$ and $v \ll \Delta_g$, where v is the vibrational mode frequency of the harmonically trapped ions' motion. The specific case in which $\Delta_g = v$, that is, tuning to the motional sideband, will be discussed later as it corresponds to coupling of the electronic degree of freedom to the motional degree of freedom.

Hyperfine states of electrodynamically trapped $^{171}\text{Yb}^+$ ions characterized by quantum numbers $F = 0$ and $F = 1$ in the electronic ground state $S_{1/2}$ are used in the experiments reported here (Methods).

After the initial preparation of an ion in the $|0\rangle$ ($F = 0$) state by optical pumping, the procedure to generate and detect dressed states can be thought of as being divided into three segments (Fig. 2, inset). First (up to time $t = T_1$), an incomplete stimulated Raman adiabatic passage[24] (STIRAP) is used to transfer the system adiabatically from the atomic-state basis to the dressed-state basis. Second (up to $t = T_2$), the amplitudes of the dressing fields are kept constant for a holding time, $T = T_2 - T_1$, because we are interested in creating and using dressed states (as opposed to population transfer). Between $t = T_1$ and $t = T_2$, dressed states are present (Fig. 1a, b, right-hand side) and quantum operations with them are implemented through application of radio-frequency fields. For a single-qubit gate between dressed
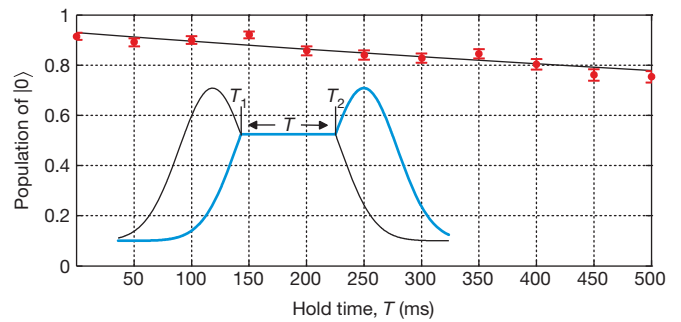
Figure 2 | Lifetime of the dressed state $|D\rangle$. To prepare the dressed state $|D\rangle$, the dressing fields' amplitudes are ramped up adiabatically until time T_1. Then these amplitudes are kept constant until time T_2. Between T_1 and T_2, the dressed states shown in Fig. 1 (right-hand side) are present. Finally, after time T_2, the STIRAP sequence is completed, adiabatically transferring the dressed state $|D\rangle$ back to a bare ionic state. The hold time is $T = T_2 - T_1$. If state $|D\rangle$ stays invariant during time T, then the final ionic state will be $|0\rangle$. The data points indicate the probability to find the ion in state $|0\rangle$ upon completion of this sequence as a function of T. The solid line represents a fitted exponential giving a lifetime of $1{,}700 \pm 300$ ms. Number of repetitions, $n = 300$; error bars, s.d. Experimental parameters are given in Supplementary Information. Inset, qualitative time dependence of the two dressing fields' amplitudes (black and blue; set on resonance with the atomic transitions $|-1\rangle \leftrightarrow |0\rangle$ and $|+1\rangle \leftrightarrow |0\rangle$).

states (Fig. 1a, right-hand side) the radio-frequency field is on resonance with the $|0'\rangle \leftrightarrow |\pm 1\rangle$ transition, and for a multiqubit gate (Fig. 1b) the radio frequency is detuned from this transition by the vibrational mode frequency, v. Third ($t > T_2$), the STIRAP sequence is completed when the ion is transferred from the dressed-state basis back to the atomic states. Any dephasing of a dressed state or transitions to other states during the holding time, T, gives rise to imperfect population transfer during step three of this sequence that returns the system to the atomic-state basis. This is described in more detail in Methods for the creation and detection of the state $|D\rangle$.

In Fig. 2, we show the effectiveness of preparation and detection of $|D\rangle$ as a function of the holding time, T. The measurement shown there extends over 500 ms and an exponential fit of the data yields a lifetime for this state of $1{,}700 \pm 300$ ms. This lifetime is limited by magnetic field fluctuations that couple $|D\rangle$ to other states and the creation of a different dark state through phase fluctuations between the two microwave fields. This represents a remarkable improvement, of more than two orders of magnitude, in the dependence on the magnetic fluctuations, as the dephasing time of the magnetically sensitive bare atomic states $|\pm 1\rangle$ in this apparatus has a measured coherence time not exceeding 5.3 ms.

We have investigated the effectiveness of the STIRAP process for creating dressed states and transferring them into the final state, as a function of the parameters characterizing the pulse sequence, and have found this technique to be robust over a wide range of experimental parameters (Methods).

To demonstrate the enhanced coherence time of this qubit, we have conducted Rabi- and Ramsey-type measurements. First, the system is transferred to the dressed-state basis and then an additional radio-frequency field with Rabi frequency Ω_g is applied that induces Rabi oscillations between the dressed states $|B\rangle$ and $|0'\rangle$. Using the state $|B\rangle$ has the advantage that no phase of π between the radio-frequency fields is needed (compare with Fig. 1). Completing the STIRAP cycle then maps the system to an atomic state that depends on the position of the atom in the dressed-state Rabi cycle. Results are shown in Fig. 3a. The Rabi oscillations are sustained over 550 ms, demonstrating the long-lived coherence of the dressed states when driven by radio-frequency radiation.

These experiments also demonstrate that coherent transfer to the dressed-state basis and subsequent application of a Rabi pulse prepares a coherent superposition in the qubit space that can then be read out
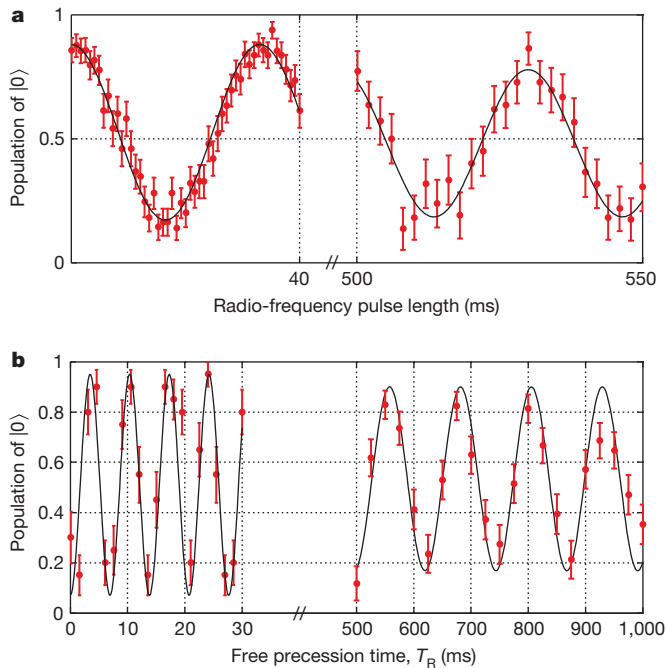
Figure 3 | Single-qubit gates with dressed states. a, Rabi oscillations between dressed state $|B\rangle$ and $|0'\rangle$, induced by a radio-frequency field for times of up to more than 500 ms. The population in $|B\rangle$ is mapped onto state $|0\rangle$ (data points) at the end of the STIRAP and detection sequence. $n = 50$ (times up to 40 ms) and $n = 25$ (times of more than 500 ms); error bars, s.d. **b**, Ramsey-type measurement preparing a coherent superposition of $|B\rangle$ and $|0'\rangle$ and probing it after time T_R, the free precession time. Two radio-frequency π/2-pulses separated by a period T_R of free evolution are applied to the qubit transition. The radio frequency is slightly detuned from resonance (near 10.265 MHz, corresponding to the $|-1\rangle \leftrightarrow |0'\rangle$ and $|+1\rangle \leftrightarrow |0'\rangle$ transitions) yielding Ramsey fringes with period 1/(144.4 Hz) between 0.1 and 30 ms of free precession time. For the measurement between 500 and 1,000 ms, the period is 1/(8.069 Hz) owing to a change in the detuning of the radio-frequency field. $n = 20$ (times up to 30 ms) and $n = 40$ (times 500–1,000 ms); error bars, s.d. Experimental parameters are given in Supplementary Information.

efficiently after completion of the STIRAP cycle. This forms the basis for the measurements of the lifetime of coherent superpositions in the protected subspace, which we now turn to.

Our Ramsey-type experiments test the dephasing time of the dressed-state qubit. Figure 3b shows that coherence is preserved for more than 1,000 ms, close to the absolute limit, of about 1,700 ms, set by the lifetime of the state $|D\rangle$ and more than two orders of magnitude longer than the dephasing time of the atomic states $|-1\rangle$ and $|+1\rangle$, making this scheme ideal for realizing a quantum memory.

Multiqubit gates can be realized by coupling the electronic qubit to the motion of the ions[10,11,26]. Several schemes for achieving such conditional quantum dynamics are possible using dressed states. Here we outline the scheme illustrated in Fig. 1b. We use a pair of radio-frequency fields on the $|0'\rangle \leftrightarrow |\pm1\rangle$ transitions (or a single radio-frequency field, depending on the choice of the phase between the dressing fields; Methods). These radio-frequency fields are detuned by v from resonance and are thus in resonance with the first motional sideband (Fig. 1b). In the dressed-state basis, this couples the $|B\rangle \leftrightarrow |0'\rangle$ (one additional field) or $|D\rangle \leftrightarrow |0'\rangle$ (two additional fields) qubit resonance of the protected subspace to the vibrational mode of the ion string. The coupling of $|D\rangle \leftrightarrow |0'\rangle$ or $|B\rangle \leftrightarrow |0'\rangle$, as appropriate, at zeroth order in the Lamb–Dicke parameter (carrier transition) will be cancelled in the rotating-wave approximation owing to the higher energy (by an amount corresponding to Ω) of $|B\rangle$ or $|D\rangle$, and $|D\rangle$ or, respectively, $|B\rangle$ will be coupled only at first order in the Lamb–Dicke parameter such that we obtain a Hamiltonian of the form (Methods)

$$H = \sqrt{2}\eta\Omega_g(|D\rangle\langle 0'|e^{i\delta t} + \text{h.c.})(b^+ - b)$$

where η is the Lamb–Dicke parameter, b and b^+ are respectively the annihilation and creation operators of the trap harmonic oscillator ('+' denotes adjoint), and h.c. denotes Hermitian conjugate. Importantly, because this gate has no carrier part, a small η value can be compensated for by increasing the radio-frequency power while obeying $\eta\Omega_g \ll v$. This will allow moderate static[5,6,12] or oscillating[7] magnetic field gradients to be used when realizing multiqubit quantum gates with radio-frequency or microwave radiation. Also, this scheme permits the realization of other types of gate, including gates with ions in thermal motion[10,11].

We now outline how the dressed-state scheme for QIP can be applied to a collection of trapped ions. The long wavelength of the microwave radiation requires the use of a static magnetic field gradient, if individual addressing in frequency space is desired. A gradient of a static or oscillating magnetic field is required for the generation of the coupling of the electronic degrees of freedom to the motional degrees of freedom when microwave or radio-frequency radiation is used for quantum gates. Therefore, this does not represent an additional experimental requirement.

In the absence of a static magnetic field gradient, a single pair of microwave-dressing fields is sufficient to dress all ions. In the presence of a static gradient, each ion would require its own pair of driving fields. This can be accomplished efficiently by using a microwave frequency comb where the frequency spacing coincides with the change in static Zeemann shift between neighbouring ions (Fig. 4). Thus, the dressed-state structure for each ion remains essentially the same as in the single-ion case resulting in robust memory. For both single-qubit gates and multiqubit gates, individual addressing is achieved by choosing the frequency of the radio-frequency field. Corrections are small under the condition that $\Omega_g \ll \Delta E_Z/\hbar$, where ΔE_Z is the difference in Zeeman shifts between two neighbouring ions and $\hbar$ is Planck's constant divided by 2π. An important advantage over the standard quantum computing scheme is that the carrier frequency and the sideband can be chosen by interference and not by setting the frequency on resonance with one of these transitions; that is, the choice is set by the phase difference between the two radio-frequency driving fields (Methods). This allows for fast multiqubit gates that are not limited by $\Omega_g \ll v$ but by $\eta\Omega_g \ll v$; that is, such gates are possible even in the presence of a small (effective) Lamb–Dicke parameter.

The insight gained in this work removes a major obstacle to laser-free QIP (but is also applicable to laser-based schemes). Furthermore, this scheme is not restricted to trapped ions and is in fact applicable to
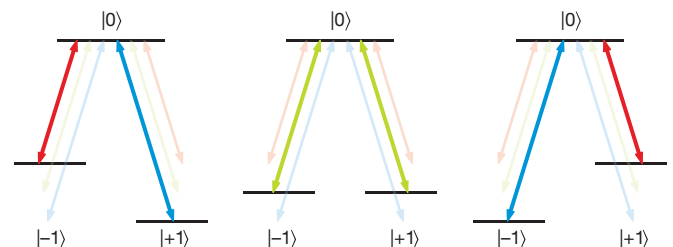
Figure 4 | Multiqubit scheme for three ions exposed to a magnetic field gradient. The magnetic field at one of the two outer ions has the same magnitude but is opposite in direction to the field at the other outer ion, producing opposite, symmetrical Zeeman energy shifts of the levels $|-1\rangle$ and $|1\rangle$. The arrows represent three pairs of microwave-dressing fields (each pair indicated by a different colour) from a comb with a frequency interval corresponding to the Zeeman shift between neighbouring ions. For each off-resonance microwave field with detuning Δ acting on a particular ion, there is a second field with equal and opposite detuning, $-\Delta$. Hence, each such off-resonance pair will couple only to either $|B\rangle$ or $|D\rangle$ (depending on the relative phase between the microwave fields) leading to equal and opposite a.c. Zeeman shifts, which then cancel.

other physical systems in which dephasing due to external perturbations has a role, for instance neutral atoms[27] and solid-state systems such as nitrogen-vacancy centres in diamond[28], ion-doped crystals[28], and circuit quantum electrodynamics[29].

METHODS SUMMARY

The experimental system. The atomic hyperfine states of the electronic ground state of the ^{171}Yb$^+$ ions used in this work can be mapped to the general scheme shown in Fig. 1 as follows: $|F=0\rangle \leftrightarrow |0\rangle$, $|F=1, m_F=-1\rangle \leftrightarrow |-1\rangle$, $|F=1, m_F=+1\rangle \leftrightarrow |+1\rangle$, $|F=1, m_F=0\rangle \leftrightarrow |0'\rangle$ (ref. 30).

The effectiveness of the STIRAP process for creating dressed states and transferring them into the final state has been investigated in detail as a function of the parameters characterizing the pulse sequence (Methods).

Single-qubit gate. We refer to $\{|0'\rangle, |D\rangle\}$ as the D qubit and to $\{|0'\rangle, |B\rangle\}$ as the B qubit in what follows. The Hamiltonian reads:

$$H_{sqg} = \omega_0|0\rangle\langle 0| + \lambda_0(|1\rangle\langle 1| - |-1\rangle\langle -1|)$$
$$+ \Omega(|-1\rangle\langle 0|e^{-i\omega_{-1}t} + e^{i\theta}|1\rangle\langle 0|e^{-i\omega_1 t} + \text{h.c.})$$
$$+ \Omega_g \cos(\lambda_0 t)(|-1\rangle\langle 0'| + \text{h.c.})$$
$$+ \Omega_g \cos(\lambda_0 t + \phi)(|1\rangle\langle 0'| + \text{h.c.})$$

Here, ω_0 is the zero-field hyperfine splitting, $\omega_{\pm 1}$ are the microwave frequencies with their initial phase difference θ, λ_0 is the radio frequency, and ϕ is the initial phase difference between the radio frequency fields. For $\theta=0$ and $\phi=\pi$ we obtain the D qubit, and for $\theta=\pi$ and $\phi=0$ we obtain the B qubit. If we set $\omega_{-1}=\omega_0+\lambda_0$ and $\omega_1=\omega_0-\lambda_0$, then by moving to the interaction picture with respect to the time-independent part we find in the rotating wave approximation (RWA), for the D qubit, that:

$$H_{sqg}^I = \sqrt{2}\Omega(|B\rangle\langle 0| + \text{h.c.}) + \sqrt{2}\Omega_g(|D\rangle\langle 0'| + \text{h.c.})$$
$$= \frac{\Omega}{\sqrt{2}}|u\rangle\langle u| - \frac{\Omega}{\sqrt{2}}|d\rangle\langle d| + \sqrt{2}\Omega_g(|D\rangle\langle 0'| + \text{h.c.})$$

The first two terms shift states $|u\rangle$ and $|d\rangle$ (which both contain $|B\rangle$) away from $|D\rangle$, and the second part creates the gate. The interactions created by the two microwave fields with Rabi frequency Ω and the radio-frequency fields of frequency Ω_g (Fig. 1a) permit the implementation of this single-qubit gate. The two radio-frequency fields have a phase difference of π at the initial time of the pulse, which realizes the coupling to $|D\rangle$ and not to $|B\rangle$.

Alternatively, we may work with the B qubit (Methods).

Multiqubit gate. The levels and fields of Fig. 1b (for the D qubit) are described by the Hamiltonian

$$H_{mqg} = \omega_0|0\rangle\langle 0| + \lambda_0(|1\rangle\langle 1| - |-1\rangle\langle -1|)$$
$$+ \Omega(|-1\rangle\langle 0|e^{-i\omega_{-1}t} + e^{i\theta}|1\rangle\langle 0|e^{-i\omega_1 t} + \text{h.c.})$$
$$+ \Omega_g \cos[(\lambda_0-\delta)t](|-1\rangle\langle 0'| + \text{h.c.})$$
$$+ \Omega_g \cos[(\lambda_0-\delta)t + \theta + \pi](|1\rangle\langle 0'| + \text{h.c.})$$
$$+ vb^+ b|1\rangle\langle 1| + \lambda(|-1\rangle\langle -1| - |1\rangle\langle 1|)(b+b^+)$$

where λ is proportional to the magnetic gradient as in ref. 6, δ is the detuning of the radio frequency field, $\theta=0$ for the D qubit and $\theta=\pi$ for the B qubit.

In the interaction picture with respect to the microwaves in RWA, and after the polaron transformation $U = e^{\eta|+1\rangle\langle +1|(b^+-b)}e^{-\eta|-1\rangle\langle -1|(b^+-b)}$, the radio-frequency part becomes

$$UHU^+ = \Omega_g(|-1\rangle\langle 0'|e^{-\eta(b^+-b)}e^{i\delta t}$$
$$+ e^{i\theta}|1\rangle\langle 0'|e^{\eta(b^+-b)}e^{i\delta t} + \text{h.c.})$$

To first order in the Lamb–Dicke parameter, for the D qubit we obtain the Hamiltonian

$$\sqrt{2}\eta\Omega_g(|D\rangle\langle 0'|e^{i\delta t} - \text{h.c.})(b^+ - b)$$

To zeroth order, we obtain a coupling between $|B\rangle$ and $|0'\rangle$; however, this term is ignored because the coupling, Ω_g, is much smaller than the energy gap, which is of order Ω. For the B qubit, we get the analogous Hamiltonian (Methods).

1. Blatt, R. & Wineland, D. Entangled states of trapped atomic ions. *Nature* **453**, 1008–1015 (2008).
2. Friedenauer, A. Schmitz, H. Glueckert, J. T., Porras, D. & Schaetz, T. Simulating a quantum magnet with trapped ions. *Nature Phys.* **4**, 757–761 (2008).
3. Kim, K. *et al.* Quantum simulation of frustrated Ising spins with trapped ions. *Nature* **465**, 590–593 (2010).
4. Gerritsma, R. *et al.* Quantum simulation of the Dirac equation. *Nature* **463**, 68–71 (2010).
5. Johanning, M. Varón, A. F. & Wunderlich, C. Quantum simulations with cold trapped ions. *J. Phys. B* **42**, 154009 (2009).
6. Mintert, F. & Wunderlich, C. Ion-trap quantum logic using long-wavelength radiation. *Phys. Rev. Lett.* **87**, 257904 (2001).
7. Ospelkaus, C. *et al.* Trapped-ion quantum logic gates based on oscillating magnetic fields. *Phys. Rev. Lett.* **101**, 090502 (2008).
8. Ozeri, R. *et al.* Errors in trapped-ion quantum gates due to spontaneous photon scattering. *Phys. Rev. A* **75**, 042329 (2007).
9. Plenio, M. B. & Knight, P. L. Decoherence limits to quantum computation using trapped ions. *Proc. R. Soc. Lond. A* **453**, 2017–2041 (1997).
10. Sørensen, A. & Mølmer, K. Entanglement and quantum computation with ions in thermal motion. *Phys. Rev. A* **62**, 022311 (2000).
11. Milburn, G. J. Schneider, S. & James, D. F. V. Ion trap quantum computing with warm ions. *Fortschr. Phys.* **48**, 801–810 (2000).
12. Wunderlich, C. in *Laser Physics at the Limit* (eds Meschede, D., Zimmermann, C. & Figger, H.) 261–271 (Springer, 2002).
13. Wunderlich, C. & Balzer, C. Quantum measurements and new concepts for experiments with trapped ions. *Adv. At. Mol. Phys.* **49**, 293–372 (2003).
14. Mc Hugh, D. & Twamley, J. Quantum computer using a trapped-ion spin molecule and microwave radiation. *Phys. Rev. A* **71**, 012315 (2005).
15. Wang, S. X. Labaziewicz, J. Ge, Y., Shewmon, R. & Chuang, I. L. Individual addressing of ions using magnetic field gradients in a surface-electrode ion trap. *Appl. Phys. Lett.* **94**, 094103 (2009).
16. Johanning, M. *et al.* Individual addressing of trapped ions and coupling of motional and spin states using RF radiation. *Phys. Rev. Lett.* **102**, 073004 (2009).
17. Häffner, H. *et al.* Robust entanglement. *Appl. Phys. B* **81**, 151–153 (2005).
18. Kielpinski, D. *et al.* A decoherence-free quantum memory using trapped ions. *Science* **291**, 1013–1015 (2001).
19. Home, J. P. *et al.* Complete methods set for scalable ion trap quantum information processing. *Science* **325**, 1227–1230 (2009).
20. Viola, L. & Lloyd, S. Dynamical suppression of decoherence in two-state quantum systems. *Phys. Rev. A* **58**, 2733–2744 (1998).
21. Rabl, P. *et al.* Strong magnetic coupling between an electronic spin qubit and a mechanical resonator. *Phys. Rev. B* **79**, 041302 (2009).
22. Biercuk, M. J. *et al.* Optimized dynamical decoupling in a model quantum memory. *Nature* **458**, 996–1000 (2009).
23. Bluhm, H. *et al.* Dephasing time of GaAs electron-spin qubits coupled to a nuclear bath exceeding 200 μs. *Nature Phys.* **7**, 109–113 (2011).
24. Vitanov, N. V. Fleischhauer, M. Shore, B. W. & Bergmann, K. Coherent manipulation of atoms and molecules by sequential laser pulses. *Adv. At. Mol. Phys.* **46**, 55–190 (2001).
25. Sørensen, J. *et al.* Efficient coherent internal state transfer in trapped ions using stimulated Raman adiabatic passage. *New J. Phys.* **8**, 261 1–11 (2006).
26. Cirac, J. I. & Zoller, P. Quantum computations with cold trapped ions. *Phys. Rev. Lett.* **74**, 4091–4094 (1995).
27. Specht, H. P. *et al.* A single-atom quantum memory. *Nature* **473**, 190–192 (2011).
28. Simon, C. *et al.* Quantum memories. *Eur. Phys. J. D* **58**, 1–22 (2010).
29. Clarke, J. & Wilhelm, F. K. Superconducting quantum bits. *Nature* **453**, 1031–1042 (2008).
30. Hannemann, T. *et al.* Self-learning estimation of quantum states. *Phys. Rev. A* **65**, 050303 1–4 (2002).

METHODS

The experimental system. The atomic hyperfine states of the electronic ground state of the ^{171}Yb$^+$ ions used in this work can be mapped to the general scheme shown in Fig. 1 as follows: $|F=0\rangle \leftrightarrow |0\rangle$, $|F=1, m_F=-1\rangle \leftrightarrow |-1\rangle$, $|F=1, m_F=+1\rangle \leftrightarrow |+1\rangle$, $|F=1, m_F=0\rangle \leftrightarrow |0'\rangle$ (ref. 30).

For STIRAP, two microwave fields with Gaussian amplitude envelopes shifted in time relative to each other are used to drive the $|-1\rangle \leftrightarrow |0\rangle$ and $|+1\rangle \leftrightarrow |0\rangle$ transitions, respectively (Fig. 1).

The effectiveness of the STIRAP process for creating dressed states and transferring them into the final state has been investigated as a function of the parameters characterizing the pulse sequence (see ref. 25 for optical STIRAP). The sequence is divided into discrete time increments $\Delta t = 1/f_\Omega N_t$, where N_t is a positive integer, $f_\Omega = \Omega_p/2\pi$ and Ω_p is the peak Rabi frequency. The width of the Gaussian pulses is given by N/f_Ω, where N is an integer. The STIRAP sequence is robust to variations of these parameters: we investigated the range $10 \leq N_t \leq 40$ for $N=10$ and found no variation in the effectiveness of the pulse sequence; that is, the overall fidelity of initial preparation of $|0\rangle$, preparation of $|D\rangle$ and read out stays constant (within statistical variations) at a value of about 93%.

When measuring sequences with pulse widths varying in the range $2 \leq N \leq 20$, equally good results were obtained for $N \geq 4$. The separation in time, s_t/f_Ω, of the two Gaussian pulses was varied over the range $0 \leq s_t/f_\Omega \leq 40/f_\Omega$, for a pulse width with $N=10$ to obtain a plateau of high effectiveness ($\sim$93%) for values of s_t in the interval $10 \leq s_t \leq 20$. The best performance is obtained for equal detunings $\Delta_+ = \Delta_-$, ideally $\Delta_+ = 0 = \Delta_-$, and for small relative detunings. For $|\delta| = |\Delta_+ - \Delta_-| < 0.1\Omega$, an experimental investigation yielded no statistically significant variation of the dressed-state preparation fidelity.

To prepare, for example, the state $|D\rangle$, the population is first transferred from the initial state $|0\rangle$ to the atomic state $|-1\rangle$ by applying a microwave π-pulse. The first half of the STIRAP sequence then transfers the atomic population to the dressed state $|D\rangle$.

A holding period in the evolution of the two STIRAP microwave fields is introduced at the crossing point of the amplitude envelopes of the two pulses. At that time, the occupation of $|D\rangle$ is at its maximum. Any dephasing of $|D\rangle$ or transitions to other states during the holding time, T, gives rise to imperfect population transfer during the second half of the STIRAP sequence that transfers the system to the atomic state $|+1\rangle$.

Probing the state after the complete STIRAP sequence does not distinguish between $|-1\rangle$ and $|+1\rangle$, as both yield bright results on final detection of resonance fluorescence. Therefore, a π-pulse swaps the populations of $|+1\rangle$ and $|0\rangle$ before final detection. Thus, a dark result indicates a successful STIRAP transfer between atomic states and dressed states, and a lifetime T of the dressed state prepared during the holding period (Fig. 2).

To record Rabi oscillations between dressed states, we first prepare state $|B\rangle$. Then a radio-frequency pulse in resonance with $|0'\rangle \leftrightarrow |\pm 1\rangle$ (Fig. 1a) is applied during the holding time, T, in the evolution of STIRAP. This radio-frequency pulse induces Rabi oscillations between $|B\rangle$ and $|0'\rangle$. After the Rabi pulse, the STIRAP pulse sequence is completed and the population of the atomic state $|0\rangle$ is probed as described above. If during the radio-frequency Rabi pulse state $|0'\rangle$ is populated, then the second part of the STIRAP sequence has no effect; that is, $|0\rangle$ is not populated at the end of the experimental sequence.

Single-qubit gate. We refer to $\{|0'\rangle, |D\rangle\}$ as the D qubit and to $\{|0'\rangle, |B\rangle\}$ as the B qubit in what follows. The Hamiltonian reads:

$$H_{sqg} = \omega_0|0\rangle\langle 0| + \lambda_0(|1\rangle\langle 1| - |-1\rangle\langle -1|)$$
$$+ \Omega(|-1\rangle\langle 0|e^{-i\omega_{-1}t} + e^{i\theta}|1\rangle\langle 0|e^{-i\omega_1 t} + \text{h.c.})$$
$$+ \Omega_g \cos(\lambda_0 t)(|-1\rangle\langle 0'| + \text{h.c.})$$
$$+ \Omega_g \cos(\lambda_0 t + \phi)(|1\rangle\langle 0'| + \text{h.c.})$$

Here, ω_0 is the zero-field hyperfine splitting, $\omega_{\pm 1}$ are the microwave frequencies with their initial phase difference θ, λ_0 is the radio frequency, and ϕ the initial phase difference between the radio frequency fields. For $\theta = 0$ and $\phi = \pi$ we obtain the D qubit, and for $\theta = \pi$ and $\phi = 0$ we obtain the B qubit. In the rotating-wave approximation we get

$$H_{sqg} = \omega_0|0\rangle\langle 0| + \lambda_0(|1\rangle\langle 1| - |-1\rangle\langle -1|)$$
$$+ \Omega(|-1\rangle\langle 0|e^{-i\omega_{-1}t} + e^{i\theta}|1\rangle\langle 0|e^{-i\omega_1 t} + \text{h.c.})$$
$$+ \Omega_g(|-1\rangle\langle 0'|e^{-i\lambda_0 t} - e^{i\theta}|1\rangle\langle 0'|e^{i\lambda_0 t} + \text{h.c.})$$

with $\theta = 0$ for the D qubit and $\theta = \pi$ for the B qubit. If we set $\omega_{-1} = \omega_0 + \lambda_0$ and $\omega_1 = \omega_0 - \lambda_0$, then by moving to the interaction picture with respect to the time-independent part we find, for the D qubit, that

$$H_{sqg}^I = \sqrt{2}\Omega(|B\rangle\langle 0| + \text{h.c.}) + \sqrt{2}\Omega_g(|D\rangle\langle 0'| + \text{h.c.})$$
$$= \frac{\Omega}{\sqrt{2}}|u\rangle\langle u| - \frac{\Omega}{\sqrt{2}}|d\rangle\langle d| + \sqrt{2}\Omega_g(|D\rangle\langle 0'| + \text{h.c.})$$

The first two terms shift states $|u\rangle$ and $|d\rangle$ (which both contain $|B\rangle$) away from $|D\rangle$, and the second part creates the gate. The interactions created by the two microwave fields with Rabi frequency Ω and the radio-frequency fields of frequency Ω_g (Fig. 1a) permit the implementation of this single-qubit gate. The two radio-frequency fields have a phase difference of π at the initial time of the pulse, which realizes the coupling to $|D\rangle$ and not to $|B\rangle$.

Alternatively, we may work with the B qubit by choosing the same initial phase for the two radio-frequency fields; that is, one radio-frequency field is sufficient to couple to $|B\rangle$. We find that

$$H_{sqg}^I = \sqrt{2}\Omega(|D\rangle\langle 0| + \text{h.c.}) + \sqrt{2}\Omega_g(|B\rangle\langle 0'| + \text{h.c.})$$
$$= \frac{\Omega}{\sqrt{2}}|u\rangle\langle u| - \frac{\Omega}{\sqrt{2}}|d\rangle\langle d| + \sqrt{2}\Omega_g(|B\rangle\langle 0'| + \text{h.c.})$$

Multiqubit gate. The levels and fields of Fig. 1b (for the D qubit) are described by the Hamiltonian

$$H_{mqg} = \omega_0|0\rangle\langle 0| + \lambda_0(|1\rangle\langle 1| - |-1\rangle\langle -1|)$$
$$+ \Omega(|-1\rangle\langle 0|e^{-i\omega_{-1}t} + e^{i\theta}|1\rangle\langle 0|e^{-i\omega_1 t} + \text{h.c.})$$
$$+ \Omega_g \cos[(\lambda_0 - \delta)t](|-1\rangle\langle 0'| + \text{h.c.})$$
$$+ \Omega_g \cos[(\lambda_0 - \delta)t + \theta + \pi](|1\rangle\langle 0'| + \text{h.c.})$$
$$+ \nu b^+ b|1\rangle\langle 1| + \lambda(|-1\rangle\langle -1| - |1\rangle\langle 1|)(b + b^+)$$

where λ is proportional to the magnetic gradient as in ref. 6, δ is the detuning of the radio frequency field, $\theta = 0$ for the D qubit and $\theta = \pi$ for the B qubit. In the rotating wave approximation, we get:

$$H_{mqg} = \omega_0|0\rangle\langle 0| + \lambda_0(|1\rangle\langle 1| - |-1\rangle\langle -1|)$$
$$+ \Omega(|-1\rangle\langle 0|e^{-i\omega_{-1}t} + e^{i\theta}|1\rangle\langle 0|e^{-i\omega_1 t} + \text{h.c.})$$
$$+ \Omega_g(|-1\rangle\langle 0'|e^{-i(\lambda_0 - \delta)t} + e^{i\theta}|1\rangle\langle 0'|e^{-i(\lambda_0 - \delta)t} + \text{h.c.})$$
$$+ \nu b^+ b|1\rangle\langle 1| + \lambda(|-1\rangle\langle -1| - |1\rangle\langle 1|)(b + b^+)$$

In the interaction picture with respect to the microwaves, and after the polaron transformation $U = e^{\eta|+1\rangle\langle +1|(b^+ - b)} e^{-\eta|-1\rangle\langle -1|(b^+ - b)}$, the radio-frequency part becomes

$$UHU^+ = \Omega_g(|-1\rangle\langle 0'|e^{-\eta(b^+ - b)}e^{i\delta t}$$
$$+ e^{i\theta}|1\rangle\langle 0'|e^{\eta(b^+ - b)}e^{i\delta t} + \text{h.c.})$$

To first order in the Lamb–Dicke parameter, for the D qubit we obtain the Hamiltonian

$$\sqrt{2}\eta\Omega_g(|D\rangle\langle 0'|e^{i\delta t} - \text{h.c.})(b^+ - b)$$

To zeroth order, we obtain a coupling between $|B\rangle$ and $|0'\rangle$; however, this term is ignored because the coupling, Ω_g, is much smaller than the energy gap, which is of order Ω. For the B qubit, we get the analogous Hamiltonian

$$\sqrt{2}\eta\Omega_g(|B\rangle\langle 0'|e^{i\delta t} - \text{h.c.})(b^+ - b)$$

When using a microwave frequency comb to dress many non-degenerate qubits, small errors due to higher-order effects may be introduced and the implementation of gates may lead to off-resonance transitions and, hence, phase shifts in other ions. However, it is important to note that the size of this error is exactly the same as for magnetic-gradient-induced coupling[6]. This is due to the fact that the microwave fields almost completely decouple the $\{|u\rangle, |d\rangle\}$ subspace from the qubit subspace ($\{|D\rangle, |0'\rangle\}$) as long as Ω is much larger (typically an order of magnitude) than the radio-frequency coupling, Ω_g.